

Comparative analysis of SHALSTAB and SINMAP for landslide susceptibility mapping in the Cunha River basin, southern Brazil

Gean Paulo Michel · Masato Kobiyama · Roberto Fabris Goerl

Received: 1 February 2013 / Accepted: 1 March 2014 / Published online: 18 March 2014
© Springer-Verlag Berlin Heidelberg 2014

Abstract

Purpose The Shallow Landsliding Stability Model (SHALSTAB) and Stability Index Mapping (SINMAP) models have been applied to various landslide management and research studies. Both models combine a hydrological model with an infinite slope stability model for predicting landslide occurrence. The objectives of the present study were to apply these two models to the Cunha River basin, Santa Catarina State, southern Brazil, where many landslides occurred in November 2008, and perform a comparative analysis of their results.

Materials and methods Soil samples were collected to determine the input parameters. The models were calibrated with a landslide scar inventory, and rainfall data were obtained from three rain gauges. A comparison of their results obtained from the models was undertaken with the success and error index.

Results and discussion Based on the maps of stability and instability areas for the study basin, the models performed well. Since the initial equations of both models are not particularly different, their results are similar. Locations with steep slopes, as well as areas with concave relief that tend to have larger contribution areas and moisture, have lower stability indexes. SHALSTAB classified only ~13 % of the total area of the Cunha River basin as unstable, while SINMAP classified ~30 % as unstable.

Conclusions The analysis of maps based on the results of the two models shows that if SHALSTAB is correctly calibrated, based on hydrological parameters, its results could be more accurate than SINMAP in the prediction of landslide areas. Although SINMAP showed better calibration of the landslide scars, its classification over the basin results in an overestimation of stability areas. The conclusion is that SHALSTAB is more suitable than SINMAP for the prediction of landslides in the Cunha River basin, Brazil.

Keywords Landslides · SHALSTAB · SINMAP · Slope stability

1 Introduction

Landslides are natural processes responsible for landscape formation and evolution, channel maintenance and sediment supply and are one of the main mechanisms for sediment release from the hillslope to the fluvial system (Cendrero and Dramis 1996; Petley 2010). Their processes and effects can be assessed and addressed in several ways, such as frequency and magnitude analysis (Steijn 1996), sediment delivery (Corsini et al. 2009) and fluvial connectivity (Crozier 2010).

As erosion processes, landslides contribute strongly to the total sediment yield and their impacts can be observed in high rates of sedimentation of reservoirs, dams and river beds (Bathurst et al. 2005). Chen et al. (2010) showed that torrential rains induced hazards in a reservoir, such as high suspended sediment concentration, which stopped the water supply, and caused floating timbers in the reservoir that shut off the power generation. Kobiyama et al. (2011) reported that in the Cubatão do Norte River basin in Brazil, an area covered by natural forests, the sediment yield due to a landslide

Responsible editor: Cristiano Poletto

G. P. Michel (✉) · M. Kobiyama
Instituto de Pesquisas Hidráulicas, Universidade Federal do Rio Grande do Sul, Avenida Bento Gonçalves, 9500, Caixa Postal, 15029, Porto Alegre, RS 91501-970, Brazil
e-mail: geanpmichel@gmail.com

R. F. Goerl
Programa de Pós Graduação em Geografia, Universidade Federal do Paraná, Centro Politécnico, Jardim das Américas, Curitiba, PR 81531-990, Brazil

occurrence was approximately five times higher than that without the phenomenon.

Despite the fact that landslide conditioning and triggering factors are well-known (Cendrero and Dramis 1996), the prediction and mapping of their occurrences are still a challenge for science and technology communities (Petley 2012). Maps of areas susceptible to landslides are important in basin management. They can provide information for the development and elaboration of risk maps and support planning of structural and non-structural measures (Korup 2005).

Bathurst et al. (2005) emphasized the need for hydrological, physically-based and spatially-distributed models to predict the occurrence of landslides and to understand their relationship with basin characteristics and sediment yield. Generally, hydrological models are coupled with slope stability models to predict landslide occurrence. Furthermore, the outputs from the coupled models can be combined with digital topography and implemented in a GIS platform. These models compute the factor of safety (*FS*) for each cell at any time during a rainstorm and incorporate the results in maps showing the *FS* values of the slopes. This type of approach allows the analysis of possible scenarios (rainfall events) with different probabilities of occurrence (Corominas and Moya 2008).

There are several stability models, such as CHASM, SHALSTAB, SINMAP, TRIGRS, SHETRAN, GEOTop-FS and SUSHI (Safaei et al. 2011). Among these models, Shallow Landsliding Stability Model (SHALSTAB) (Dietrich and Montgomery 1998) and Stability Index Mapping (SINMAP) (Pack et al. 1998) have a similar construction that utilise hydrological, geomorphic and geotechnical features and involve the same input parameters. Although similar, SHALSTAB has a deterministic approach, while SINMAP is probabilistic.

The objectives of the present study were, therefore, to: (1) summarize SHALSTAB and SINMAP, (2) apply them to the Cunha River basin, Santa Catarina State, Brazil and (3) perform a comparative analysis of the results obtained with these two models. There are some investigations that have compared SHALSTAB and SINMAP (e.g. Meisina and Scarabelli 2007; Andriola et al. 2009). However, since both models are very important for landslide management, it is still necessary to carry out this type of comparison with different regional characteristics.

2 Theory

2.1 Infinite slope stability model

Since shallow landslides, in which the slope length is greater than the soil depth, occur frequently in Brazil, the infinite slope stability model can be very useful. This model compares the destabilizing and restorative components on a plane

parallel to the soil surface, ignoring the edge effect. The infinite slope stability model (Fig. 1) is based on the Mohr-Coulomb law in which, at the moment of failure, the shear stress, τ (N m^{-2}), due to the downslope component of the soil weight, is equal to the resistance strength caused by cohesion, c (N m^{-2}), and by frictional resistance due to the effective normal stress on the failure plane:

$$\tau = c + (\sigma - u) \cdot \tan \phi \tag{1}$$

where σ is the normal stress (N m^{-2}); u is the pore pressure opposing the normal load (N m^{-2}); and ϕ is the angle of internal friction of the soil (degrees).

Selby (1993) proposed a modification to Eq. (1) for an infinite slope:

$$\rho_s \cdot g \cdot z \cdot \sin \theta \cdot \cos \theta = c_r + c_s + (\rho_s \cdot g \cdot z \cdot \cos^2 \theta - \rho_w \cdot g \cdot h \cdot \cos^2 \theta) \cdot \tan \phi \tag{2}$$

where ρ_s is the wet soil density (kg m^{-3}), z is the soil depth (m), θ is the slope (degrees), ρ_w is the water bulk density (kg m^{-3}), h is the water level (m), c_r is the root cohesion (N m^{-2}), c_s is the soil cohesion (N m^{-2}) and g is the gravitational acceleration (m s^{-2}). It is noted that the wet soil density parameter is used due to its similarity to field conditions when a landslide is triggered.

Dividing the portion of the equation (right side of Eq. (2)) that represents the soil structuring forces by the portion of the equation that represents the destabilizing forces (left side), the *FS* of the infinite slope can be obtained:

$$FS = \frac{c_r + c_s + (\rho_s \cdot g \cdot z \cdot \cos^2 \theta - \rho_w \cdot g \cdot h \cdot \cos^2 \theta) \cdot \tan \phi}{\rho_s \cdot g \cdot z \cdot \sin \theta \cdot \cos \theta} \tag{3}$$

In this equation, $FS=1$ is a balanced state, i.e. failure is imminent; at $FS < 1$, slope failure takes place and at $FS > 1$, the slope is stable. It must be noted that this value does not represent absolute stability or instability. The stability increases with an increase of *FS* values (Selby 1993).

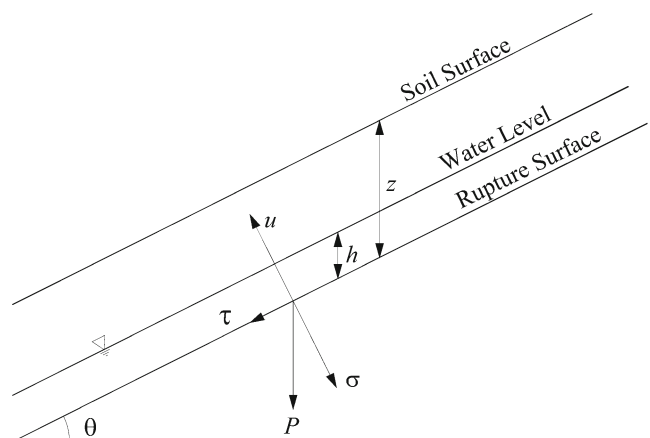


Fig. 1 Representation of an infinite slope model. *P* represents the weight of the soil block. See text for definition of symbols

The decrease of FS occurs with an increase of the water column due to the reduction of effective stress. Thus, during a rainfall event, the water table elevation reduces FS . The higher the intensity and the longer the duration of the rainfall event, the higher the probability of slope failure.

2.2 Steady-state hydrological model

The slope stability/instability condition is directly related to hydrological factors; therefore, it is essential to have a hydrological model to estimate soil moisture. The commonest hydrological concept adopted for modelling slope stability is the steady-state shallow subsurface flow which is described in TOPMODEL (Beven and Kirkby 1979) and TOPOG (O'Loughlin 1986). This concept assumes a uniform recharge state that simulates the spatial moisture variation (water level) during a rainfall event. Figure 2 demonstrates this concept, where a (m^2), b (m) and q (m d^{-1}) represent the upslope drainage area, the contour length and the recharge uniform rate, respectively.

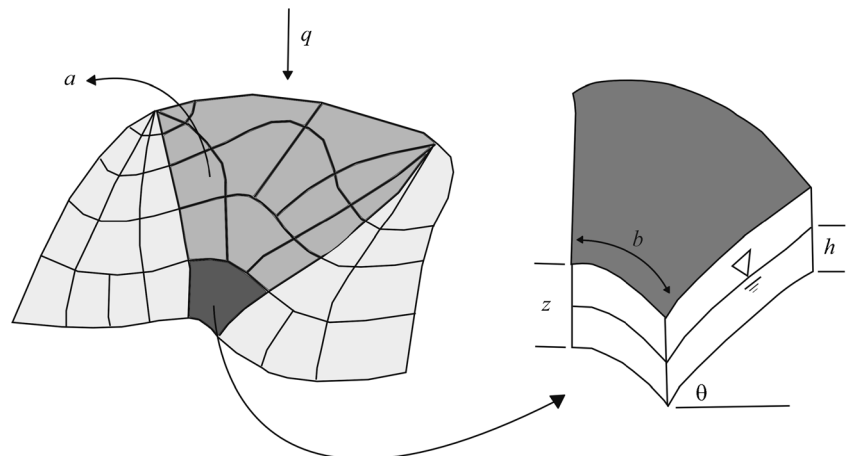
Defining the wetness as the portion of saturated soil submitted to a uniform recharge state, O'Loughlin (1986) proposed that it is given by the relation between the water inlet in the form of uniform recharge and the water outlet that exits through the soil saturated layer. Equation (4) shows the final formulation of the steady-state hydrological model.

$$W = \frac{q \cdot a}{b \cdot T \cdot \sin \theta} = \frac{h}{z} \quad (4)$$

$$\therefore T = K_s \cdot z \cdot \cos \theta \quad (5)$$

where W is the soil wetness (m m^{-1}), T is the soil transmissivity ($\text{m}^{-2} \text{d}^{-1}$) and K_s (m d^{-1}) is the saturated hydraulic conductivity, considered homogeneous along the soil depth.

Fig. 2 Representation of hydrological model (after Montgomery and Dietrich 1994)



2.3 Shallow Landsliding Stability Model (SHALSTAB)

The Shallow Landslide Stability Model (SHALSTAB) is a deterministic and distributed model based on a combination of infinite slope and steady-state hydrological models. SHALSTAB is integrated into a GIS (ArcView 3.2) through which the upslope drainage area, elevation and slope values are calculated by using a digital elevation model (DEM), and these values are assigned to each pixel.

Solving Eq. (2) in terms of h/z (saturated soil layer) results in the saturation amount necessary for the landslide to occur:

$$\frac{h}{z} = \frac{\rho_s}{\rho_w} \left(1 - \frac{\tan \theta}{\tan \phi} \right) + \frac{c}{\cos^2 \theta \cdot \rho_w \cdot g \cdot z} \quad (6)$$

Applying Eq. (6) to a slope, two extreme conditions are established: unconditionally unstable and unconditionally stable. The first condition takes place when h/z is set to 0 (absence of water column), and the relation between the soil parameters cannot compensate the destabilizing effect of the steep slope (Eq. (7)). The second condition happens when h/z is set to 1 (totally saturated), and the relation between the soil parameters overcomes the effect of the slope (Eq. (8)).

$$\tan \theta \geq \tan \phi + \frac{c}{\cos^2 \theta \cdot \rho_s \cdot g \cdot z} \quad (7)$$

$$\tan \theta \leq \tan \phi \cdot \left(1 - \frac{\rho_w}{\rho_s} \right) + \frac{c}{\cos^2 \theta \cdot \rho_s \cdot g \cdot z} \quad (8)$$

When the unconditionally unstable and stable conditions are not established, a partial soil saturation can lead to slope failure, and Eqs. (4) and (6) can be equated. Thus, the infinite

slope and steady-state hydrological models are coupled:

$$\frac{q \cdot a}{T \cdot b \cdot \sin\theta} = \frac{\rho_s}{\rho_w} \left(1 - \frac{\tan\theta}{\tan\phi} \right) + \frac{c}{\cos^2\theta \cdot \tan\phi \cdot \rho_w \cdot g \cdot z} \tag{9}$$

A modification of Eq. (9) in terms of the parameters q and T generates the final formulation of SHALSTAB:

$$\frac{q}{T} = \frac{b}{a} \cdot \sin\theta \cdot \left\{ \frac{\rho_s}{\rho_w} \left(1 - \frac{\tan\theta}{\tan\phi} \right) + \frac{c}{\cos^2\theta \cdot \tan\phi \cdot \rho_w \cdot g \cdot z} \right\} \tag{10}$$

The input parameters required by SHALSTAB are c , φ , ρ_s and z . The other variables (a , b and θ) are extracted from the DEM. Therefore, SHALSTAB classifies the terrain as a function of a hydrologic ratio (q/T) required to instability. Dietrich and Montgomery (1998) originally proposed seven stability classes. The most extreme classes—unconditionally unstable and unconditionally stable—are related to Eqs. (7) and (8), and the other five classes are established as a function of q/T .

2.4 Stability Index Mapping (SINMAP)

The Stability Index Mapping (SINMAP) is a stochastic and distributed model that is used for mapping slope stability. Like SHALSTAB, this model also applies a steady-state hydrological model coupled to an infinite slope model (Pack et al. 1998). SINMAP is also a GIS-integrated (ArcGIS 9.2) model. The topographic variables are obtained from the DEM. SINMAP derives its terrain stability classification from topographic, hydrological and soil characteristics. An uncertainty range can be established for the hydrological and soil parameters.

By assuming uniform distributions of the parameters over uncertainty ranges, this model calculates, as the principal output, the Stability Index (SI) which is defined as the probability that a location is stable. This value normally ranges between 0 (most unstable) and 1 (least unstable). However, at places where the most conservative (destabilizing) set of parameters in the model still results in stability, the SI values become >1 . The stability classes adopted by SINMAP are shown in Table 1.

SINMAP is based on Eq. (3) to calculate the FS . The steady-state hydrological model (Eq. (11)) is used to estimate soil saturation, assuming that the maximum value of h/z is equal to 1. Then, if the value is >1 , overland flow is formed.

$$W = \frac{h}{z} = \text{Min} \left(\frac{q \cdot a}{T \cdot b \cdot \sin\theta}, 1 \right) \tag{11}$$

The q/T rate determines the relative wetness in terms of uniform recharge state in relation to soil capability in drain

water. Although the term “steady-state” is used to name the model, the q value does not represent a long-term average of recharge (e.g. annual). It is a rate of effective recharge, for a critical period, required to trigger landslides (Pack et al. 1998).

By replacing Eq. (11) with Eq. (3) and rearranging, the final formulation of SINMAP is established:

$$FS = \frac{c_a + \cos\theta \cdot \left[1 - \text{Min} \left(\frac{q \cdot a}{T \cdot b \cdot \sin\theta}, 1 \right) \cdot r \right] \cdot \tan\phi}{\sin\theta} \tag{12}$$

where c_a is the dimensionless cohesion ($c_a = \frac{c_r + c_s}{\rho_s \cdot g \cdot z \cdot \cos\theta}$), and r is the relation between water and wet soil density ($r = \frac{\rho_w}{\rho_s}$). Some input parameters of SINMAP are described in terms of maximum and minimum thresholds, like T/q (m), c_a and φ (degrees). For ρ_s , only its mean value is used.

Random variations of the input parameters between their boundaries generate a probability distribution of terrain stability (probability of $FS > 1$). Assuming that the variable T/q is represented by x , then x_1 is the lower boundary and x_2 is the upper boundary. Likewise, by representing $\tan \phi$ by t , then t_1 and t_2 are the lower and the upper boundary, respectively; similarly, c_1 and c_2 represent the lower and upper boundary of the dimensionless cohesion, respectively.

The worst scenario (most conservative) is the combination of the lower values of c and t (c_1 and t_1) with the highest x value (x_2):

$$SI = FS_{\min} = \frac{c_1 + \cos\theta \cdot \left[1 - \text{Min} \left(x_2 \frac{a}{b \cdot \sin\theta}, 1 \right) \cdot r \right] \cdot t_1}{\sin\theta} \tag{13}$$

Under this condition, if $FS > 1$, the location is considered unconditionally stable. At any locations where the minimum FS is <1 , there is a failure probability. In this case, the SI is defined as:

$$SI = \text{Prob}(FS > 1) \tag{14}$$

The best scenario combines the upper boundary of c and t (c_2 and t_2) with the lower boundary of x (x_1). Thus, the maximum value of FS is obtained:

$$SI = FS_{\max} = \frac{c_2 + \cos\theta \cdot \left[1 - \text{Min} \left(x_1 \frac{a}{b \cdot \sin\theta}, 1 \right) \cdot r \right] \cdot t_2}{\sin\theta} \tag{15}$$

Under this condition, if $FS < 1$, the location is considered unconditionally unstable.

Table 1 Stability classes in the SINMAP model

Stability index	Stability classes	Parameter range	Possible influence of factors not modelled
$SI > 1.5$	Unconditionally stable	Range cannot model instability	Significant destabilizing factors are required for instability
$1.5 > SI > 1.25$	Moderately stable	Range cannot model instability	Moderate destabilizing factors are required for instability
$1.25 > SI > 1.0$	Quasi-stable	Range cannot model instability	Minor destabilizing factors could lead to instability
$1.0 > SI > 0.5$	Lower threshold of stability	Pessimistic half of range required for instability	Destabilizing factors are not required for instability
$0.5 > SI > 0.0$	Upper threshold of stability	Optimistic half of range required for stability	Stabilizing factors may be responsible for stability
$0.0 > SI$	Unconditional instability	Range cannot model instability	Stabilizing factors are required for stability

Modified from (Pack et al. 1998)

3 Materials and methods

3.1 Study area description

In November 2008, an extreme rainfall event triggered floods and landslides in Santa Catarina state, Brazil, especially in the Itajaí Valley. The town of Rio dos Cedros, in the Itajaí Valley, was declared a state of public calamity due to this rainfall event. In this city, 8,561 people (83 % of the total population) were directly affected. The floods occurred in the urban area and the landslides, mainly debris flows, occurred in rural areas (Kobiyama et al. 2010).

Four large landslides and three other minor ones were recorded in the Cunha River basin (16.35 km²), in which this town is located (Fig. 3). The Cunha River basin is 70 % covered by dense rainforest and another 20 % is covered by pasture. Among the seven significant landslides, six were triggered in forested areas and one in pasture. Therefore, the present study chose this basin for a comparative analysis of the SHALSTAB and SINMAP models.

This basin varies from 90 to 860 m a.m.s.l., with a mean slope of 8 %. The basin is composed of gneiss (94 %) and shale (6 %). The inceptisols, classified as cambisols by the Brazilian System of Soil Classification (EMBRAPA 2009), are predominant and occupy about 75 % of the basin (IBGE 2003). These soils are mainly associated with steep slopes and are composed of clayey material in this basin. The other 25 % of the basin is occupied by ultisols (classified as argisols in the Brazilian classification).

3.2 Input parameters

3.2.1 Topographic data

The DEM was made using 5 m-counter lines obtained in a survey with a Leica ADS-40 sensor set-up in an airplane. The Topo to Raster toolbox in ArcGis 9.3 was used to interpolate the contour and to create the DEM with a pixel resolution of 5 m. The DEM was used to determine the slope and drainage

area at each point. Slope values decrease with coarser DEM resolutions (Claessens et al. 2005; Wu et al. 2008). The higher the topographic resolution, the more accurately the map reproduces the drainage area and slope (Dietrich et al. 2001). Dietrich et al. (2001) performed SHALSTAB validation using 10-m grids and suggested that the grid size influences the critical uniform recharge rate. Although there is no such thing as a ‘perfect’ DEM resolution, and no resolution can represent the dimensions of all the possible slope failures (Claessens et al. 2005), the resolution adopted by the present study possibly represents the more significant landslides that occurred in the basin.

The landslide scars were determined by visual analysis of the basin orthophotos (1:5,000 scale). Furthermore, several points of the landslide crown scars were measured using a Differential GPS Trimble R3 and 5700 and a Leica TPS-407 total station. By delineating the scars and by identifying their source, transport and deposition areas, a landslide inventory map was made and used to calibrate the models. In the present study, the area delimited by the inventory considered only the source of the landslides. The transport and depositional areas were not treated.

3.2.2 Rainfall data

The hourly rainfall data obtained at three rain gauge stations located in the town of Rio dos Cedros (Fig. 3) were converted to a daily uniform recharge rate. The extension of the rainfall period was determined by Michel et al. (2011). A uniform recharge rate of 15.33 mm day⁻¹ was adopted as input data. No evidence of rills, ravines or any overland flow was observed during the field survey. Therefore, it was assumed that no significant overland flow occurs in the basin and, consequently, that the soil recharge rate is equal to the rainfall intensity.

3.2.3 Soil data

Soil samples were collected at 10 sites inside the landslide source areas whose soil characteristics represent the slope

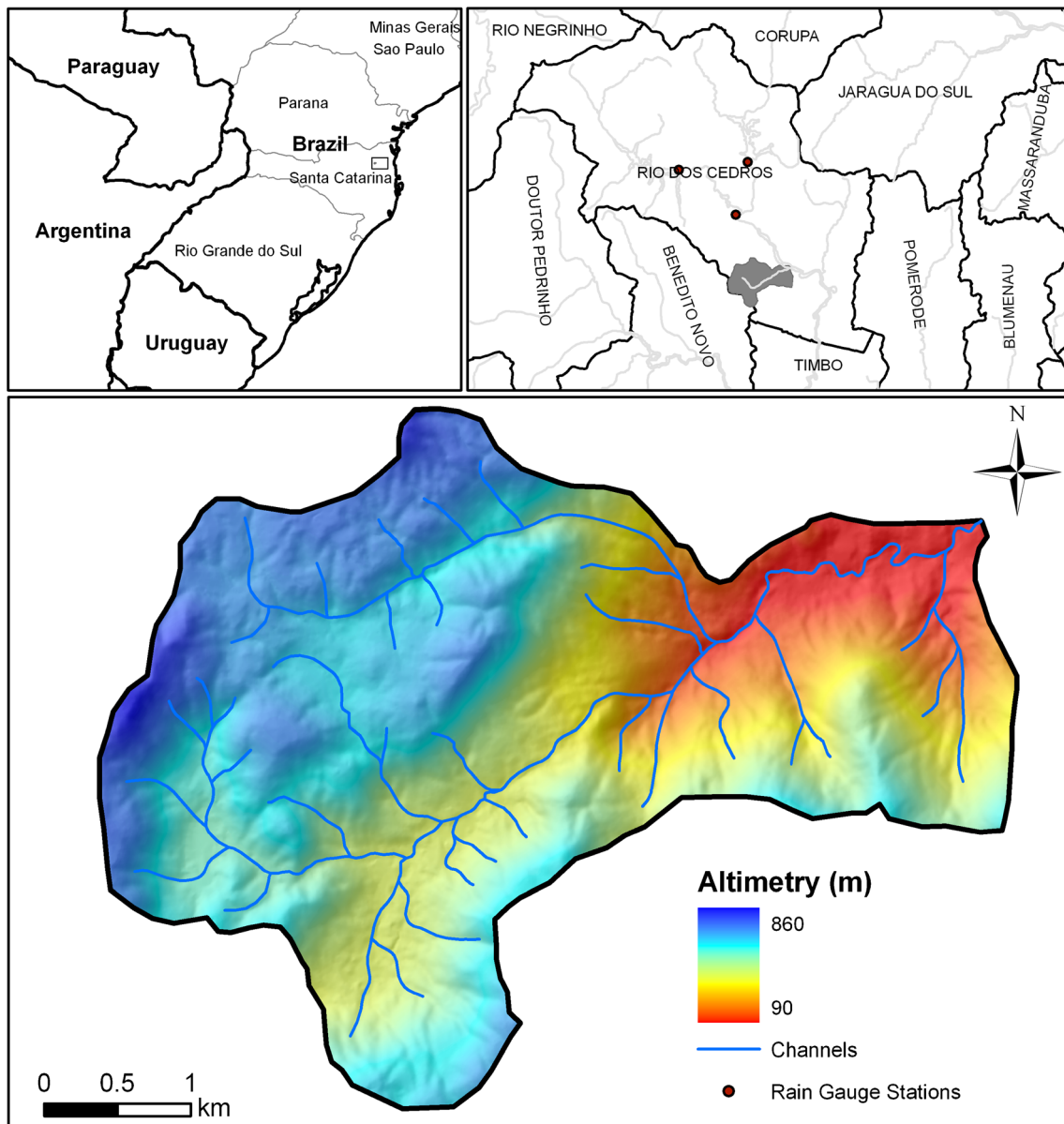


Fig. 3 Location and altimetry of the Cunha River basin, Brazil

failure conditions. Laboratory tests were carried out on the soil samples to obtain the shear strength parameters, density and particle size distribution of the soil. The shear strength parameters of soil (φ and c) were determined by the direct shear test with undisturbed soil samples. The value of ρ_s was determined from the relation between mass and volume of the wet undisturbed soil.

Due to the difficulty of performing the K_s tests in situ because the landslides occurred at very steep and remote localities, the particle size distribution of soil samples was used to estimate K_s by the HYDRUS-1D software that contains the Rosetta Lite Version 1.1 model proposed by Schaap et al. (2001). The K_s values estimated by HYDRUS-1D are, on average, one order of magnitude smaller than those measured

by Schaap and Leij (2000); Mota and Kobiyama (2011) compared the values of K_s measured in the laboratory with those estimated by HYDRUS-1D of some Brazilian soils whose sampling locations are very close to the present study. They reported that the values of K_s estimated by HYDRUS-1D were, in general, 10 to 100 times smaller than the measured ones. To take into account the HYDRUS-1D estimation uncertainty, the value of K_s adopted by the present study was 10 times larger than the estimated one. Though the K_s value generally decreases with depth of forest soils, the present study considered its value constant. The soil depth was estimated through field observations of the landslide scars. The value adopted for the entire basin was considered equal to the soil depth where the slope failure occurred.

The mean value of each parameter is presented in Table 2. Since SHALSTAB is a deterministic model, the values of Table 2 were used directly. As a stochastic model, SINMAP requires the maximum and minimum parameter values. Thus, their values vary by $\pm 20\%$.

3.2.4 Model calibration

Model calibration is normally carried out by evaluating the spatial coincidence between mapped landslide scars and simulated unstable areas. The more coincidences are observed, the better a calibration performance is considered. An usual calibration procedure is to vary the input parameters by increasing the spatial coincidence between landslide scars and simulated unstable areas. However, this procedure may result in large unstable areas over the entire basin, which can be unrealistic. Thus, the variation of the input parameters should be done carefully. Since the soil data were obtained from laboratory tests with samples collected in a field and the obtained values possess less uncertainty, the model calibration was undertaken by changing the uniform recharge rate (hydrological parameter). This procedure was described in detail by Michel et al. (2011).

3.2.5 Efficiency evaluations of the models

The efficiency of the models was evaluated with two indexes proposed by Sorbino et al. (2010): index (*SuI*) and error index (*ErI*) (Fig. 4). *SuI* represents the percentage of area considered as unstable by the model (A_{in}) within the real landslide scar area (A_{unst}) while *ErI* is the percentage rate between the unstable areas defined by the model outside the landslide scar (A_{out}) and the basin area that was not affected by the landslides (A_{stab}):

$$SuI = \frac{A_{in}}{A_{unst}} \cdot 100 \quad (16)$$

$$ErI = \frac{A_{out}}{A_{stable}} \cdot 100 \quad (17)$$

Furthermore, Sorbino et al. (2010) suggested calculating the ratio between *SuI* and *ErI* in the case of similar values

Table 2 Mean value of each soil parameter

Parameter	Mean value
Internal friction angle of soil (φ)	31.2°
Cohesion (c)	11.9 kPa
Saturated hydraulic conductivity (K_s)	3.8 m day ⁻¹
Wet soil density (ρ_s)	1,815 kg m ⁻³
Soil depth (z)	10 m

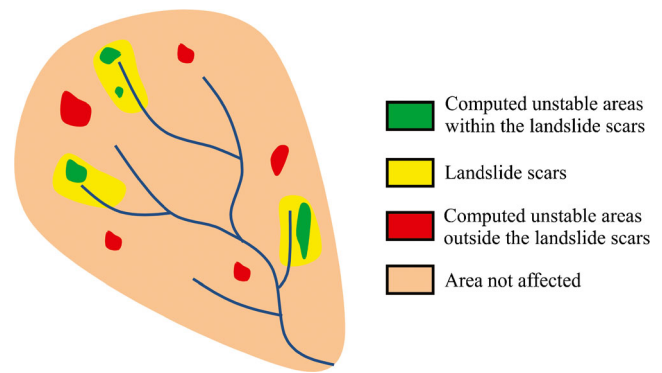


Fig. 4 Conceptual illustration of success and error indexes (after Sorbino et al. 2010)

between these indices. The higher ratio indicates the better performance of the model.

4 Results and discussion

4.1 SHALSTAB

Figure 5 shows the results of the SHALSTAB simulation, i.e. a stability map of the Cunha River basin with the seven different classes as established by Dietrich and Montgomery (1998). All the gentle and plane areas were classified as stable, even in saturation conditions. Areas with a steep slope are strongly related to instability, even in areas of poor saturation condition. It is noted that the upslope drainage area has a strong influence on the terrain stability classification. At the flow accumulation locations where the slope is convergent, there is a relatively high concentration of unstable areas.

All the landslide scars are identified in two higher instability classes in Fig. 5. Among the mapped landslides, one coincided with the unconditionally unstable class and the other six with the second class of higher instability. On the other hand, only 12.84 % of the total area of the Cunha River basin was identified as these unstable classes. Therefore, the SHALSTAB calibration was considered satisfactory for the Cunha River basin. Table 3 presents the area distribution for each class and the number of landslides per class. The stability classification was determined as a function of $\log q/T$. Thus, hydrological parameters were used to estimate the slope saturation, which consequently permitted the calculation of its stability degree. The spatial correlation between the mapped landslide scars and the two most unstable classes, and the small area classified as these two classes over the whole basin, indicate that SHALSTAB correctly described the hydrogeomorphological effects on slope instability for the Cunha River basin.

When a place is classified as unconditionally unstable, some specific conditions need to be addressed, for example

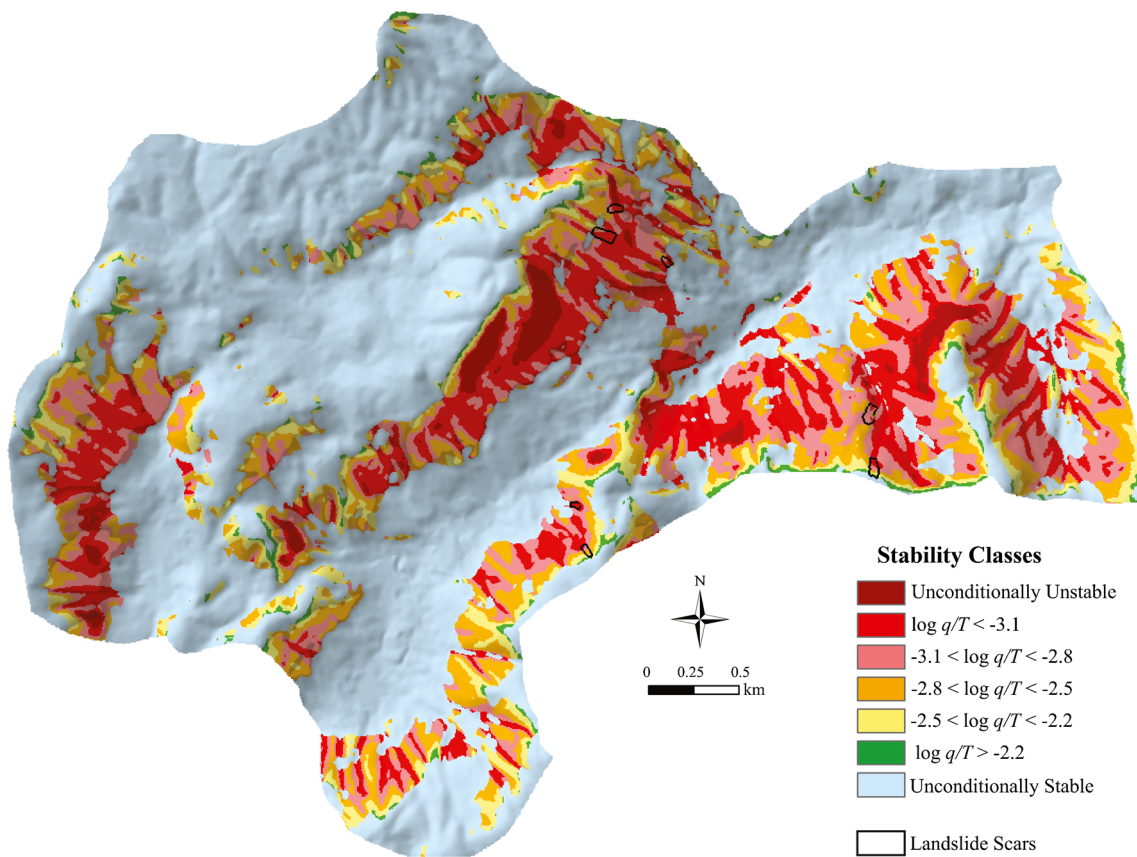


Fig. 5 Stability map obtained from the SHALSTAB model

a substantial soil layer on a steep slope. However, this particular situation is not usually observed naturally because steep slopes normally suffer from high rates of surface erosion. Therefore, this situation, as described by the mathematical model, is not consistent with the real world.

4.2 SINMAP

The stability map resulting from SINMAP simulation is characterized with six classes for the studied basin (Fig. 6). Each

class represents the range of *SI* which in turn represents the probability for each pixel to obtain an *FS* > 1. Since the initial equations of SINMAP and SHALSTAB are not very different, their results are quite similar. Locations with steep slopes, as well as the concave relief that tend to have larger contribution areas and higher soil moisture, have lower stability indexes.

The recorded landslide scars coincide with the three classes of lower stability, where, according to SINMAP classification, the *SI* value is < 1. None of the recorded landslides were identified as unconditionally unstable. Similar to an

Table 3 Landslide and areas per stability class

Classes	Area (km ²)	Area (%)	Number of landslides	Landslides (%)
Uncond. unstable	0.23	1.43	1	14.29
$\log q/T < -3.1$	1.85	11.41	6	85.71
$-3.1 < \log q/T < -2.8$	1.73	10.67	0	0.00
$-2.8 < \log q/T < -2.5$	1.69	10.45	0	0.00
$-2.5 < \log q/T < -2.2$	0.91	5.65	0	0.00
$\log q/T > -2.2$	0.20	1.21	0	0.00
Uncond. stable	9.58	59.18	0	0.00
Total	16.2	100.00	7	100.00

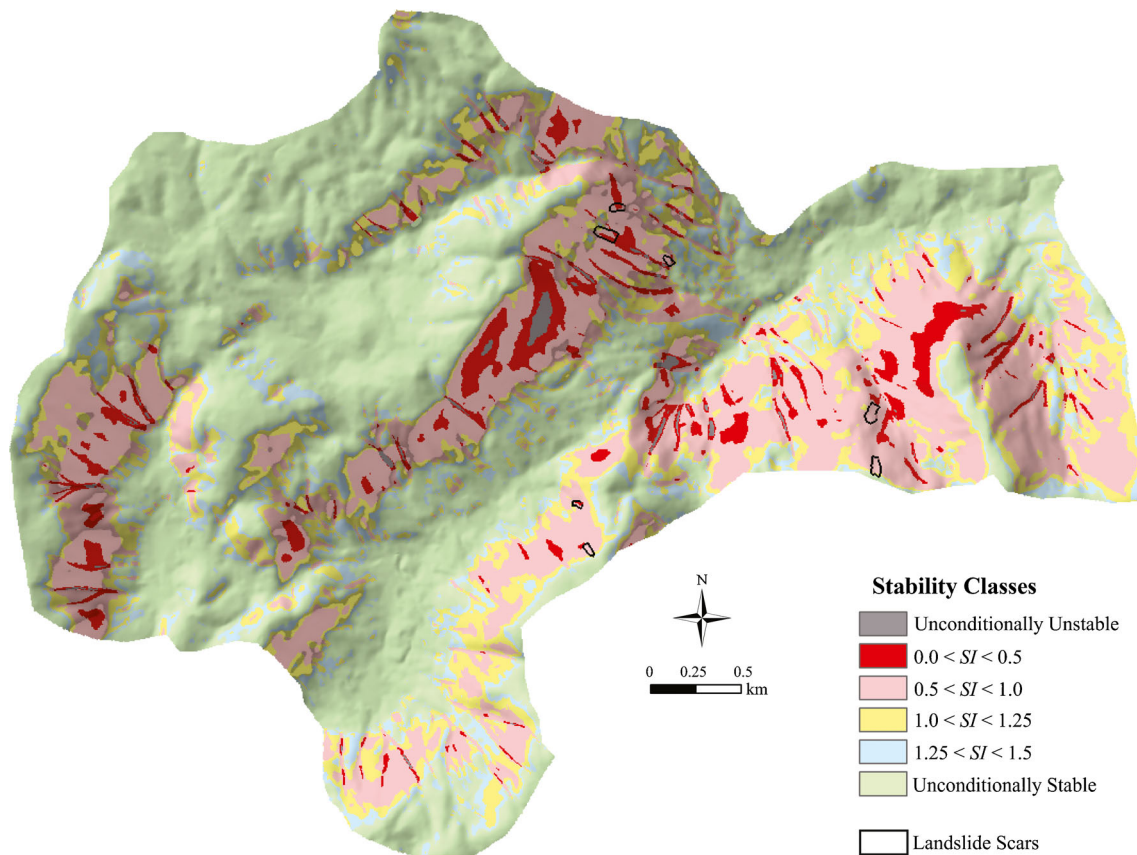


Fig. 6 Stability map obtained from the SINMAP model

interpretation of the SHALSTAB simulation result, this class requires a certain specific condition that does not commonly occur in the real world.

The class with the largest number of landslides is the upper threshold of stability ($0.0 < SI < 0.5$) with five landslide scars in this class, followed by the lower threshold of stability with two landslide scars (Table 4). The 71.43 % of correspondence between the second more unstable class and landslide scars and also the classification of only 4.4 % of the basin area as this class of SINMAP indicated that the calibration was satisfactory. On the other hand, to match all the landslides inside the unstable classes, SINMAP classified 30 % of the entire basin as unstable.

4.3 Comparison

To perform a comparative analysis of the models, two criterions were established. In SHALSTAB, unconditionally unstable and $\log q/T < -3.4$ classes were merged into a single unstable class. Similarly, for SINMAP, the unconditionally unstable class and the classes where the value of $SI < 1$ were merged into a single class. Then by using these two new classes, the values of Sul and ErI were calculated from the maps obtained by both models.

Even with the similar initial equations, the values of Sul and ErI from SHALSTAB and SINMAP are very different

Table 4 Different stability classes and landslide occurrence distribution

Classes	Area (km ²)	Area (%)	Number of landslides	Landslides (%)
Uncond. unstable	0.03	0.20	0	0.00
$0.0 < SI < 0.5$	0.71	4.40	5	71.43
$0.5 < SI < 1.0$	4.16	25.70	2	28.57
$1.0 < SI < 1.25$	2.43	15.00	0	0.00
$1.25 < SI < 1.5$	1.80	11.10	0	0.00
Uncond. stable	7.08	43.60	0	0.00
Total	16.2	100.00	7	100.00

Table 5 Success and error indexes for the SHALSTAB and SINMAP simulation results

	SHALSTAB	SINMAP
Success index (<i>Sul</i>) (%)	19.55	94.12
Error index (<i>ErI</i>) (%)	6.35	30.22

(Table 5). The calibration processes for SHALSTAB resulted in a reduction of unstable areas in the Cunha River basin until the point that only a few unstable pixels could be found inside the landslide scar. Consequently, the calibration generated a small value of *ErI* because a few locations were classified as unstable over the basin. Furthermore the *Sul* value was also small, compared with the value obtained with SINMAP.

Since SINMAP is a probabilistic model, its simulation results refer to a probability of failure. In other words, the probabilistic distribution makes several combinations in the input parameters, which causes a tendency to classify a relatively large area in the basin, as unstable. Thus, the value of *Sul* is very high (94 %) in the SINMAP simulation. On the other hand, SINMAP has also a high value of *ErI*, which means that a lot of the areas identified as unstable do not coincide with the landslide scars.

According to Sorbino et al. (2010), a higher value of the *Sul/ErI* relation indicates a better performance of a model. For the SHALSTAB and SINMAP calibrations, the *Sul/ErI* values were 3.08 and 3.11, respectively. Therefore, the SINMAP model has a better performance than SHALSTAB for the Cunha River basin. However, the *Sul/ErI* values of the two models were very similar. Thus, it is not appropriate to make such a conclusive statement about model performance. In fact, there is a question as to whether all the areas inside the landslide scar can be considered unstable. The absence of

witnesses and other kinds of records makes it very difficult to say exactly where the movement began. Thus, only a few areas (pixels) inside the scar could be really unstable, and relaxation of tensions after the beginning of the movement could propagate the instability to the surrounding areas, resulting in a large landslide area. Therefore, there is some uncertainty in applying the *Sul/ErI* relation which is based on the unstable area inside the scar.

According to Dietrich et al. (2001), the best results of a slope stability model are gained when the landslide scars coincide with the unstable areas and at the same time these unstable areas represent a minor area over the whole basin. Figure 7 presents the cumulative percentage of the area and landslides in each stability class. In the SHALSTAB case, all the landslides coincide with the unconditionally stable and $\log q/T < -3.4$ classes (Fig. 7a). In a reclassification of the stability map by considering these two classes as unstable, only 6 % of the area of the basin was unstable. On the other hand, in the case of SINMAP, the landslides were included in the unconditionally unstable, $0.0 < SI < 0.5$ and $0.5 < SI < 1.0$ classes (Fig. 7b). Grouping these three classes in a single unstable class, 30 % of the total area of the basin was classified as unstable. In the comparative map, the area considered as unstable by both models represents 6 % of the total basin area, while the stable area identified by both represents 70 % (Fig. 8). The areas characterized as SHALSTAB stable/SINMAP unstable are encountered in 24 % of the total area. Thus, for each single pixel classified as unstable by SHALSTAB, there are about five SINMAP unstable pixels.

From the analysis of maps made with the two models, if SHALSTAB is correctly calibrated based on hydrological parameters (q/T), its results could be used more accurately in the prediction of landslide areas. Although SINMAP showed better calibration related to landslide scars, its classification over the basin results in an overestimation of stability areas.

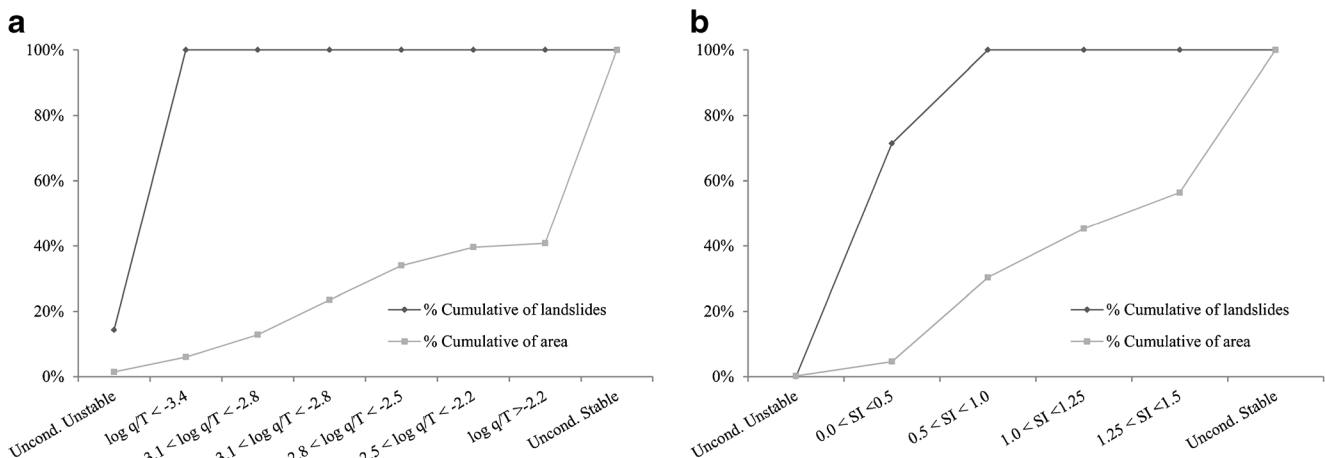


Fig. 7 Cumulative percentage of the area of landslide scars and the area of each stability class. **a** SHALSTAB and **b** SINMAP

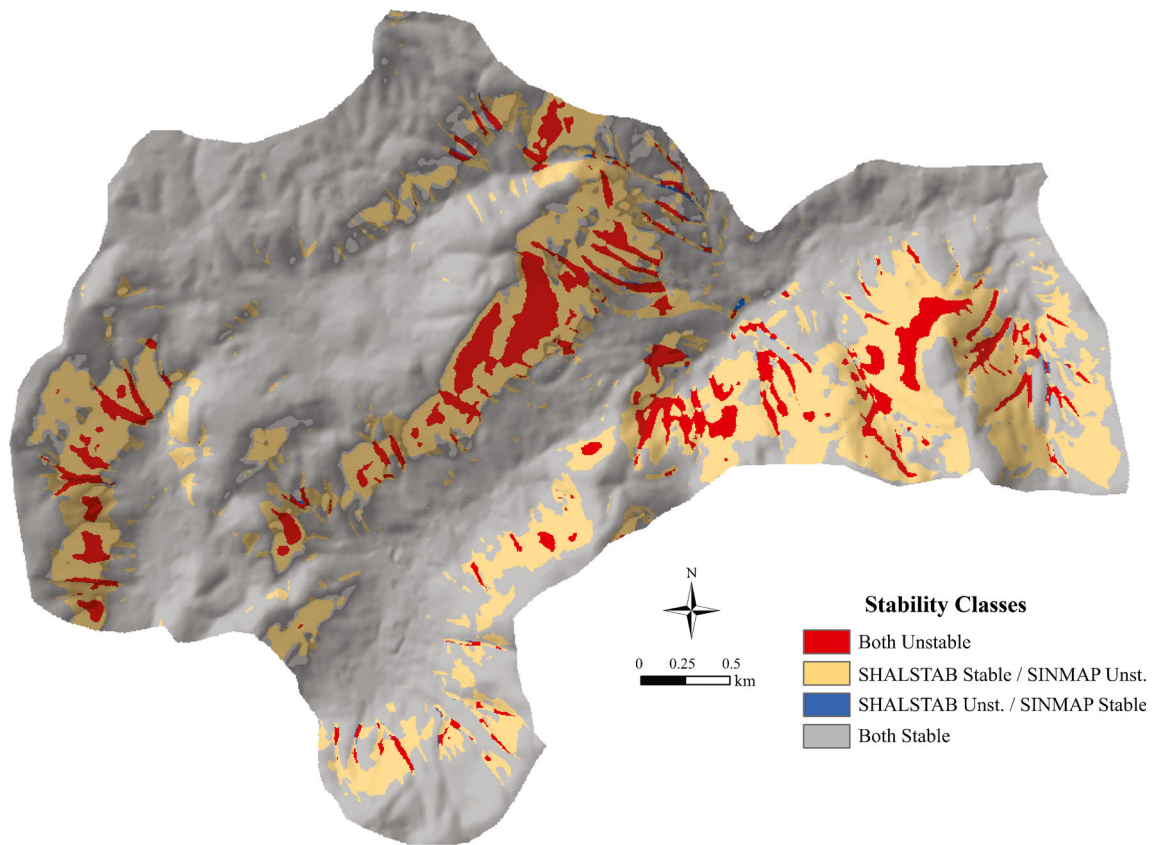


Fig. 8 Comparative map between stable and unstable areas as determined by SHALSTAB and SINMAP

Therefore, SINMAP should be applied at the preliminary assessment stage or for the first approach to landslide management.

The SHALSTAB results appropriately represent topographic and hydrological factors that control landslide occurrences. Thus, all landslide scars match unstable classes and the basin was not classified excessively as unstable. Thus, SHALSTAB is recommended over SINMAP for predicting landslides in the Cunha River basin.

5 Conclusions

The present study compared two slope stability models, SHALSTAB and SINMAP, by mapping areas susceptible to landslides (stability and instability areas) in the Cunha River basin, Brazil. The results obtained from the simulation of both models are satisfactory for the prediction of landslides in this basin. All landslide scars matched the SHALSTAB and SINMAP unstable classes.

In a comparative analysis, the best values of S_{ul}/ErI obtained from maps generated with SHALSTAB and SINMAP were 3.08 and 3.11, respectively. Reclassifying the stability map to match all landslide scars with the unstable classes,

SHALSTAB obtained better results than SINMAP. Only 6 % of the total area of the basin was classified as unstable by SHALSTAB, while 30 % was classified by SINMAP.

Besides the uncertainties related to the difficult determination of the values of the input parameters—because of their heterogeneous distribution over the basin and also related to topographic features that the DEM cannot perfectly represent—stochastic models such as SINMAP possess a certain range for each input parameter. This can potentially increase the uncertainty of the results. The SHALSTAB model is more able to identify specific areas prone to shallow landslides and can be used by managers as an additional tool in fieldwork. The conclusion is that SHALSTAB is better than SINMAP in predicting landslides in the Cunha River basin.

It is important to mention that the values of all input parameters of both models contain uncertainties. The greater the number of soil samples and laboratory tests, the more appropriate is the representation of parameter variability over the basin; however, the description cannot be perfect. The present study confirms that, because of the actual difficulty in recognizing the subsurface conditions that dictate pore-pressure evolution and material strength, no slope failure model can predict a landslide with certainty at high spatial and temporal resolution (Wilcock et al. 2003).

References

- Andriola P, Chirico GB, De Falco M, Crescenzo G, Santo A (2009) A comparison between physically-based models and a semiquantitative methodology for assessing susceptibility to flowslides triggering in pyroclastic deposits of southern Italy. *Geogr Fis Dinam Quat* 32:213–226
- Bathurst JC, Moretti G, El-Hames A, Moaven-Hashemi A, Burton A (2005) Scenario modelling of basin-scale, shallow landslide sediment yield, Valsassina, Italian Southern Alps. *Nat Hazards Earth Syst Sci* 5:189–202
- Beven KJ, Kirkby MJ (1979) A physically based, variable contributing area model of basin hydrology. *Bull Hydrol Sci* 24:43–69
- Cendrero A, Dramis F (1996) The contribution of landslides to landscape evolution in Europe. *Geomorphology* 15:191–211
- Chen CY, Chen LK, Yu FC, Lin SC, Lin YC, Lee CL, Wang YT (2010) Landslides affecting sedimentary characteristics of reservoir basin. *Environ Earth Sci* 59:1693–1702
- Claessens L, Heuvelink GBM, Schoorl JM, Veldkamp A (2005) DEM resolution effects on shallow landslide hazard and soil redistribution modelling. *Earth Surf Proc Landforms* 30:461–477
- Corominas J, Moya J (2008) A review of assessing landslide frequency for hazard zoning purposes. *Eng Geol* 102:193–213
- Corsini A, Borgatti L, Cervi F, Dahne A, Ronchetti F, Sterzai P (2009) Estimating mass-wasting processes in active earth slides—earthflows with time-series of high-resolution DEMs from photogrammetry and airborne LiDAR. *Nat Hazards Earth Syst Sci* 9:433–439
- Crozier MJ (2010) Landslide geomorphology: an argument for recognition, with examples from New Zealand. *Geomorphology* 120:3–15
- Dietrich WE, Montgomery DR (1998) SHALSTAB: a digital terrain model for mapping shallow landslide potential. NCASI (National Council of the Paper Industry for Air and Stream Improvement), Technical Report, 29 p
- Dietrich WE, Bellugi D, Real de Asua R (2001) Validation of the shallow landslide model, SHALSTAB, for forest management. In: Wigmosta MS, Burges SJ (ed) *Land use and watersheds: human influence on hydrology and geomorphology in urban and forest areas*. *Water Sci Appl*, AGU, Washington DC, vol 2 pp 195–227
- EMBRAPA Centro Nacional de Pesquisa de Solos (2009) Sistema brasileiro de classificação de solos. EMBRAPA-SPI, Rio de Janeiro, 412 p
- IBGE Gerencia de Recursos Naturais e Estudos Ambientais (2003) Reconhecimento de Solos (mapa). Folha Blumenau. Escala 1: 100000
- Kobiyama M, Goerl RF, Correa GP, Michel GP (2010) Debris flow occurrences in Rio dos Cedros, Southern Brazil: meteorological and geomorphic aspects. In: Wrachien D, Brebbia CA (eds) *Monitoring, simulation. Prevention and remediation of dense debris flows III*. WIT Press, Southampton, pp 77–88
- Kobiyama M, Almeida AA, Grison F, Giglio JN (2011) Landslide influence on turbidity and total solids in Cubatão do Norte River, Santa Catarina, Brazil. *Nat Hazards* 59:1077–1086
- Korup O (2005) Large landslides and their effect on sediment flux in South Westland, New Zealand. *Earth Surf Proc Landforms* 30:305–323
- Meisina C, Scarabelli S (2007) A comparative analysis of terrain stability models for predicting shallow landslides in colluvial soils. *Geomorphology* 87:207–223
- Michel GP, Goerl RF, Kobiyama M, Higashi RAR (2011) Estimativa da quantidade de chuva necessária para deflagrar escorregamentos. In: *Anais do XIX Simpósio Brasileiro de Recursos Hídricos*. Maceió: ABRH, 2011. CD-rom. 20 p
- Montgomery DR, Dietrich WE (1994) A physically based model for the topographic control on shallow landsliding. *Water Resour. Res.* 30:1153–1170
- Mota AA, Kobiyama M (2011) Avaliação da dinâmica da água na zona vadosa em solos de diferentes usos com o modelo Hydrus-1D. In: *XIX Brazilian Symposium of Water Resources*, Maceió, ABRH, Proceedings, 16 p
- O’Loughlin EM (1986) Prediction of surface saturation zones in natural catchments by topographic analysis. *Water Resour Res* 22: 794–804
- Pack RT, Tarboton DG, Goodwin CN (1998) Terrain stability mapping with SINMAP, technical description and users guide for version 1.00. Report Number 4114–0, Terratech Consulting Ltd., Salmon Arm, Canada, 68 p
- Petley D (2010) Landslide hazards. In: Alcantara-Ayala I, Goudie A (eds) *Geomorphological hazards and disaster prevention*. Cambridge University Press, Cambridge, pp 63–74
- Petley D (2012) Global patterns of loss of life from landslides. *Geol* 40: 927–930
- Safaei M, Omar H, Huat BK, Yousof ZBM, Ghiasi V (2011) Deterministic rainfall induced landslide approaches, advantage and limitation. *Electron J Geotech Eng* 16:1619–1650
- Schaap MG, Leij FJ (2000) Improved prediction of unsaturated hydraulic conductivity with the Mualem-van Genuchten model. *Soil Sci Soc Am J* 64:843–851
- Schaap MG, Leij FJ, van Genuchten MT (2001) Rosetta: a computer program for estimating soil hydraulic parameters with hierarchical pedotransfer functions. *J Hydrol* 251:163–176
- Selby M (1993) *Hillslope materials and processes*. Oxford University Press, Oxford, 289 p
- Sorbino G, Sica C, Cascini L (2010) Susceptibility analysis of shallow landslides source areas using physically based models. *Nat Hazards* 53:313–332
- Steijn H (1996) Debris-flow magnitude-frequency relationship of mountainous regions of Central and Northwest Europe. *Geomorphology* 15:256–273
- Wilcock PR, Schmidt JC, Wolman MG, Dietrich WE, Dominick D, Doyle MW, Grant GE, Iverson RM, Montgomery DR, Pierson TC, Schilling SP, Wilson RC (2003) When models meet managers: examples from geomorphology. In: Wilcock PR, Iverson RM (eds) *Prediction in geomorphology*, *Geophys Monogr Ser*, vol 135. AGU, Washington, pp 27–40
- Wu S, Li J, Huang GH (2008) A study on DEM-derived primary topographic attributes for hydrologic applications: sensitivity to elevation data resolution. *Appl Geogr* 28:210–223